

Effect of Temperature and Concentration on the Physical Properties of Cholesteryl Pelargonate Near Transition Temperatures

V. Gajghate^{1*}, A. Kanwar²

¹Pillai HOC College of Engineering and Technology, Khalapur, HOC Colony Rd, Taluka, Rasayani, 410207 (Maharashtra), India

²Vivekanand Education Society's College of Arts, Science and Commerce, Sindhi Society, Chembur, Mumbai-71, India

Received 9 November 2020, accepted in final revised form 28 March 2021

Abstract

Thermodynamic and acoustical study of cholesteric liquid crystal (CLC) was carried out near phase transition temperatures using an ultrasonic interferometer. The study of ultrasonic waves and related thermo-acoustical parameters provides information in understanding the nature of molecular interactions associated with liquid crystals. A statistical mechanical approach is used to calculate the viscosity of samples. The characteristic textures and phase transition temperatures are obtained with Polarizing Microscopy (POM). Fabry Perot scattering studies (FPSS) are used to ascertain the phase transition temperatures of CLC. The thermo-acoustical parameters have been calculated using experimental data with well-known formulae. The acoustical parameters show variation with temperature as well as with concentration of CLC. Anomalous behavior of these parameters is noticed at the clearing temperature of CLC. The variation of the parameters is explained in terms of solute-solvent molecular interactions in the solution. The molecular behavior, structural changes, and intermolecular interactions between CLC and solvent are discussed in detail.

Keywords: Cholesteric liquid crystal; Polarizing microscopy; Fabry Ferot scattering studies; Ultrasonic interferometer.

© 2021 JSR Publications. ISSN: 2070-0237 (Print); 2070-0245 (Online). All rights reserved.
doi: <http://dx.doi.org/10.3329/jsr.v13i2.50151> J. Sci. Res. **13** (2), 483-493 (2021)

1. Introduction

Liquid crystal is the mesomorphic phase with properties intermediate between that of a crystalline solid and an isotropic liquid. In the case of thermotropic liquid crystals, phase changes are temperature dependent. These liquid crystals respond to changes in temperature by changing colors. With the increase in temperature, their color changes from red to orange, yellow, green, and blue. The anisotropy of liquid crystals causes them to exhibit birefringence. A birefringent material placed between crossed polarizing filters shows striking patterns and color effects. Due to the helical structure, CLC possesses special optical and physical properties, which are directly responsible for technological

* Corresponding author: vishakha.deogade@gmail.com

applications. The optical properties of liquid crystals are best studied with the help of polarizing microscopy and Fabry Perot scattering studies [1]. Cholesteric liquid crystals are non-ferroelectric and exhibit blue phases between the cholesteric phase and isotropic region. The three distinct blue phases that can appear are blue phase I (BPI), blue phase II (BP II), and blue phase III (BP III). BPI and BP II show cubic symmetry whereas BP III is amorphous. One of the most striking features of the blue phases is the mosaic of reflecting colors that they display. The wavelength of reflecting color depends on the lattice structure, which includes the Miller indices of a crystal plane, average refractive index, and lattice constant of blue phases. It is found that the external electric field distorts the cubic lattice of blue phases and results in a change in the angular positions of Bragg reflection. The modulation of the lattice structure by the electric field reveals the selectivity of the reflecting color wavelengths during Bragg reflection. This exceptional property of blue phases can be used to design functional materials and devices for applications in displays and sensors [1-3]. The physical properties of liquid crystals are greatly influenced by the intermolecular forces. Ultrasonic waves are longitudinal waves with frequencies greater than 20,000 Hz. Ultrasonic waves propagate through the liquid crystal with different velocities at different temperatures and for different concentrations of liquid crystal. The study of ultrasonic velocities and their influence on molecular structure were carried out by several researchers [4,5]. Gabrielli and Verdini [6] were the first to investigate ultrasonic velocity and absorption in p-azoxyanisole, and reported abrupt variation of these acoustical parameters at the isotropic-nematic phase transition. The subsequent study by different researchers [7,8] also observed an abrupt change of acoustic parameters at the phase transition temperatures of cholesteric liquid crystals. Anomalous behavior of physical parameters was observed near the phase transition temperatures and at clearing temperature. Ultrasonic studies in a mixture of CLC and solvent were carried by an ultrasonic interferometer. Various acoustical parameters were calculated using ultrasonic velocity [9,10]. The study of ultrasonic waves and related thermo-acoustical parameters provides information regarding the nature and strength of forces existing between the molecules [11,12]. The viscosity of material strongly depends on the molecular environment. The knowledge of viscosity plays an important role in designing the processes that involve equipment design, heat transfer, and molecular dynamics. Unlike an experimental method, a statistical mechanical approach is used to calculate the viscosity of the samples. It is used to establish relationships between various physical properties of the cholesteric liquid crystal [13].

In the present work, we have studied the dependence of ultrasonic velocity and various acoustic parameters such as acoustic impedance, adiabatic compressibility, intermolecular free path length, relative association, relaxation time, ultrasonic attenuation, Rao's constant, and Wada constant of cholesteric liquid crystal solutions by varying temperatures and concentration. The measurements of ultrasonic velocity were made at various temperatures using an ultrasonic interferometer working at the frequency 1 MHz. The results obtained are analyzed to see the effect of temperature and concentration on the

ultrasonic parameters of CLC near transition temperatures and phase changes. The transition temperatures of CLC are detected using FPSS and POM.

2. Materials and Methods

2.1. Cholesteryl pelargonate

Cholesteryl Pelargonate (CP), a thermotropic liquid crystal having

Molecular formula: $C_{36}H_{62}O_2$

Molar mass: 526.88 g/mol

Pure CP has melting point between $74^{\circ}C$ - $77^{\circ}C$

Cholesteryl Pelargonate, obtained from Sigma–Aldrich, is used in the preparation of the samples. A homogeneous mixture of various concentrations of CP with toluene (T) is used as a sample to study the effect of temperature and concentration on the acoustical behavior of cholesteric liquid crystals. The samples were weighed using an electronic balance having a resolution of 10^{-3} g.

2.2. Fabry Perot scattering studies

Fabry Perot scattering studies is useful in detecting accurately the phase transition temperatures of liquid crystals. The experimental set-up consists of a Fabry-Perot Etalon coupled with the spectrometer and a source of He-Ne laser of low output power. In a liquid crystal, when a phase transition occurs, then the orientation order and/or the positional order changes. This in turn scatters the incident laser light and changes the angle of incidence of the light falling on the FP etalon. This changes the diameter of the FP rings. The changes in the diameter occur at the phase transition temperature and indicate a mesophase transition. The variation of diameter of the Fabry Perot rings with temperature is recorded. The graph indicates sudden changes in the FP rings diameter. This sudden change indicates phase transition temperatures. The technique of FPSS is used for the characterization of thermotropic liquid crystals and their mixture [15,16]. The smallest changes in the orientation and phases are recorded perfectly by this technique. The same is confirmed with the changes in ultrasonic velocity at various temperatures.

2.3. Polarizing microscopy

Polarizing microscopy is the most powerful tool for the identification of textures and confirmation of phase transition temperatures. It consists of two polarizers placed at right angles to each other. When polarized light passes through the CLC, it splits the polarized light into extraordinary and ordinary components. These two components, when travels through the analyzer interfere with each other producing colorful images. These colorful images or textures are the fingerprints that help us identify the type of mesophase liquid crystal is in, thereby revealing phase transition temperatures. Each liquid crystal phase exhibits a distinct optical texture when viewed under polarizing microscopy [17,18]. Different images of Cholesteryl Pelargonate were captured for each phase during the

heating and cooling cycles. The textures and the phase transition temperatures of CP were recorded using the POM.

2.4. Ultrasonic interferometer

The ultrasonic interferometer was used for the measurements of the velocity of ultrasonic waves in the CLC solution. In an ultrasonic interferometer, ultrasonic waves of known frequency are produced by a quartz crystal. These waves are reflected by a movable metallic plate parallel to the quartz plate. Then they superimpose and standing waves are produced in the liquid medium if the separation between these plates is exactly the whole multiple of the sound wavelength. It is a device used to determine the ultrasonic velocity of liquids and liquid mixtures with great accuracy. It has a high-frequency generator and a measuring cell. The temperature surrounding the measuring cell was kept constant in an electronically controlled thermostatic water bath, accuracy up to 0.01 K. The measurements were made at frequency 1 MHz. The least count of the micrometer measuring cell is 0.01 mm. The accuracy of ultrasonic velocity is equal to $\pm 0.5\%$. The ultrasonic velocity obtained is used to find the acoustic impedance, intermolecular free path length relative association, ultrasonic attenuation, relaxation time, Rao's constant, and Wada constant [9,10].

3. Formulae

The various acoustical parameters are calculated using following formulae

1. Viscosity (η) can be evaluated by an equation [13],

$$\frac{\eta}{\sigma} = \frac{16}{15} \sqrt{\frac{M}{RT}}$$

where σ is the surface tension of the sample, η is viscosity of solution, M is the molecular mass of the sample, T is the temperature in kelvin

Surface Tension (S) has been determined using formula:

$$v = (S/6.3 \times 10^{-4} \rho)^{2/3}$$

where v is the ultrasonic velocity of the sample, ρ is the density of the sample

2. Acoustic impedance (Z) is determined using equation [14],

$$Z = \rho v$$

where ρ is the density of the sample, v is the ultrasonic velocity of the sample

3. Intermolecular free path length (L_f) has been determined as follows [14],

$$L_f = K \beta^{\frac{1}{2}}$$

where K is the temperature dependent Jacobson's constant

($K = 205.35 \times 10^{-8}$ at 300 K),

β is the adiabatic compressibility given by $\beta = \frac{1}{\rho v^2}$

4. Relative Association (RA) can be evaluated by an equation [14],

$$RA = \left(\frac{\rho}{\rho_0}\right) \left(\frac{v_0}{v}\right)$$

where ρ_o and v_o are the density and velocity of the solvent

5. Ultrasonic attenuation ($\frac{\alpha}{f^2}$) can be evaluated by an equation [14],

$$\frac{\alpha}{f^2} = \frac{8 \eta \pi^2}{\rho v^3}$$

6. Relaxation time (τ) is calculated using the formula [14],

$$\tau = \frac{4\eta}{3\rho v^2}$$

7. Rao's constant or molar sound velocity is given by an equation [9],

$$R = \frac{M}{\rho} v^{\frac{1}{3}}$$

where $M = M_1W_1 + M_2W_2$ (M_1 and M_2 are molecular weights of CP and toluene respectively and W_1 and W_2 are weight fractions of CP and toluene respectively in the solution

8. Wada Constant or molar compressibility (W) is given by an equation [9],

$$W = \frac{M}{\rho} \beta^{-\frac{1}{7}}$$

4. Results

Cholesteryl Pelargonate when heated undergoes phase transition exhibiting two melting points, 75 °C and 92.4 °C. The various transition phases observed using polarizing microscopy is as follows:

Crystal-smectic 77.5 °C; Smectic-cholesteric 79 °C; Cholesteric-blue phase 85 °C; Cholesteric-isotropic 92.4 °C

The images of the textures of Cholesteryl Pelargonate observed through polarizing microscopy are captured using a Nikon camera for both heating and cooling cycles of the CLC. The images are shown in Fig. 1. The phase transition temperatures of CP detected with technique Fabry Perot scattering studies during heating and cooling of the sample are shown in Table 1. The variation of angular diameters of Fabry Perot rings with temperature is shown in Fig. 2. A comparison of the observations of PTTs of CP obtained with POM and FPSS is shown in Table 2. It is seen that the PTTs of CP for both techniques are approximately the same; however, more transition temperatures are observed with FPSS than that of POM. The ultrasonic velocities and the viscosity of the samples in SI units are mentioned in Table 3. Acoustic impedance, intermolecular free path length, relative association, relaxation time, Rao's constant, and Wada constant are determined using well-known formulae. The graphical variation of these acoustical parameters with temperature and concentration is shown in Figs. 3-6.

4.1. Textures of cholesteryl pelargonate

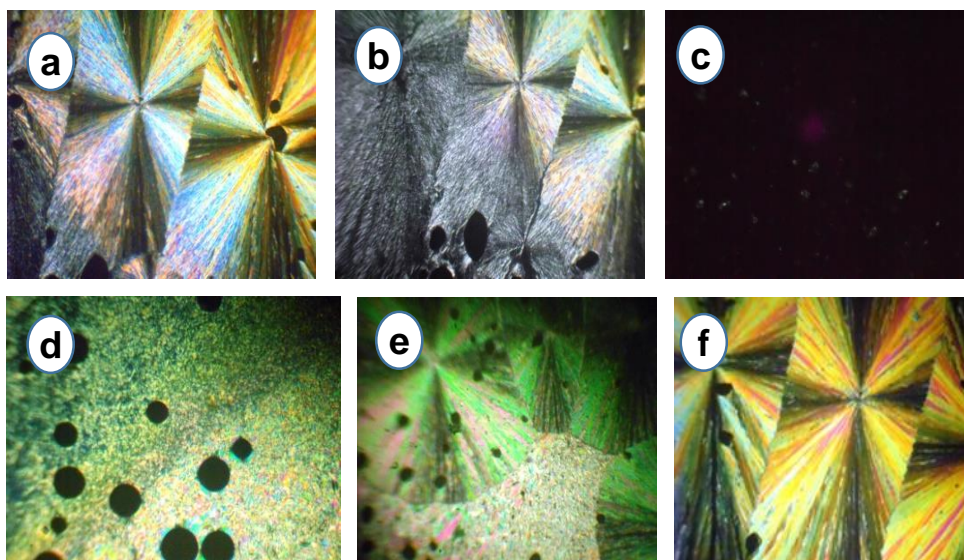


Fig. 1. Polarizing microscopic images of textures of different phases of Cholesteryl Pelargonate during the heating cycle: a) melting Point (75 °C), b) smectic phase (77.5 °C), c) isotropic phase (92.4 °C) and during the cooling cycle d) blue phase (85 °C), e) transformation to crystalline phase (40 °C) and f) at room temperature.

4.2. Determination of phase transition temperatures using FPSS

Table 1. PTT's of CP using FPSS during heating and cooling cycles of samples.

Material-CP	Heating cycle									Cooling cycle			
Temperature (°C)	40	66	68	74	78	84	88	90	92	92	90	88	74

4.3. Comparison of phase transition temperatures (in C) of CP using FPSS and POM

Table 2. PTT's of CP using FPSS and POM

Material-CP	FPSS									POM			
Heating cycle	40	66	68	74	78	84	88	90	92	75	77.5	79	92.4
Cooling cycle	92	90	88	74	-	-	-	-	-	90	85	40	-

4.4. Ultrasonic velocity and viscosity of the sample

The measured values of ultrasonic velocity and calculated values of viscosity for the samples at different temperatures are shown in the table below:

Table 3. Ultrasonic velocity and viscosity of the samples.

Temp (C)	Ultrasonic velocity in m/s				Viscosity in N/m ² s			
	T+5 mg CP	T+10 mg CP	T+15 mg CP	T+20 mg CP	T+5 mg CP	T+10 mg CP	T+15 mg CP	T+20 mg CP
76	1095.6	1097.0	1099.0	1101.0	0.000308	0.000309	0.00031	0.000311
77.5	1091.4	1092.5	1095.6	1097.8	0.000306	0.000306	0.000308	0.000309
78	1085.7	1088.6	1091.1	1093.3	0.000303	0.000304	0.000306	0.000307
79	1082.9	1085.7	1088.9	1091.1	0.000302	0.000303	0.000304	0.000305
80	1080.0	1082.9	1084.4	1086.0	0.0003	0.000301	0.000302	0.000303
81	1078.0	1080.0	1082.0	1084.0	0.000299	0.0003	0.0003	0.000301
82	1074.0	1076.0	1077.0	1079.0	0.000297	0.000298	0.000298	0.000299
83	1070.0	1072.0	1074.0	1076.0	0.000295	0.000295	0.000296	0.000297
84	1063.0	1065.0	1067.0	1068.0	0.000293	0.000294	0.000295	0.000296
85	1061.0	1062.7	1064.4	1066.0	0.00029	0.000291	0.000292	0.000292
86	1055.0	1057.9	1059.0	1062.0	0.000287	0.000288	0.000289	0.00029
87	1053.0	1055.0	1057.0	1059.0	0.000286	0.000287	0.000288	0.000289
88	1052.0	1054.0	1056.0	1058.0	0.000285	0.000286	0.000287	0.000288
89	1051.4	1052.0	1054.0	1056.0	0.000285	0.000285	0.000286	0.000286
90	1038.0	1040.0	1042.2	1044.0	0.000283	0.000283	0.000284	0.000285
91	1035.0	1037.0	1040.0	1042.0	0.000277	0.000278	0.000279	0.00028
92.4	1012.0	1014.0	1015.0	1017.0	0.000267	0.000268	0.000269	0.00027
93	1037.0	1039.0	1041.0	1042.0	0.000277	0.000278	0.000279	0.000279
94	1028.0	1032.0	1034.0	1035.0	0.000273	0.000275	0.000276	0.000276
95	1024.0	1026.0	1028.0	1029.0	0.000271	0.000272	0.000273	0.000273

4.5. Graphs of FPSS

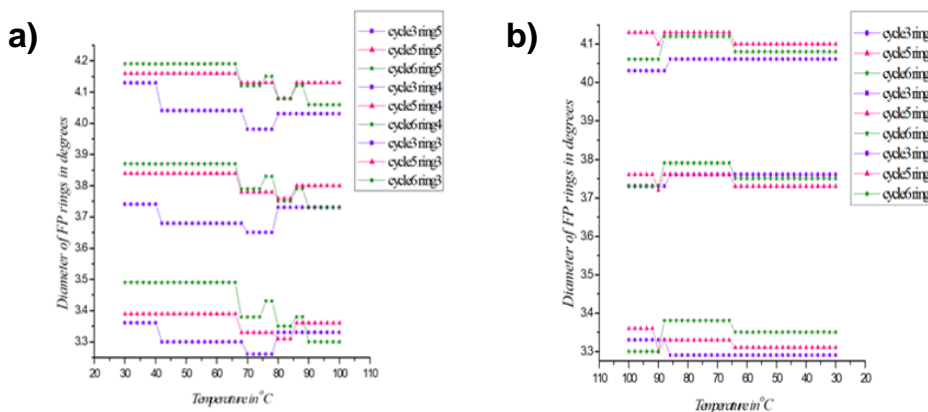


Fig. 2. The angular diameter Vs. temperature for a) heating and b) cooling cycles.

4.6. Graphical variation of the acoustical parameters with temperature and concentration

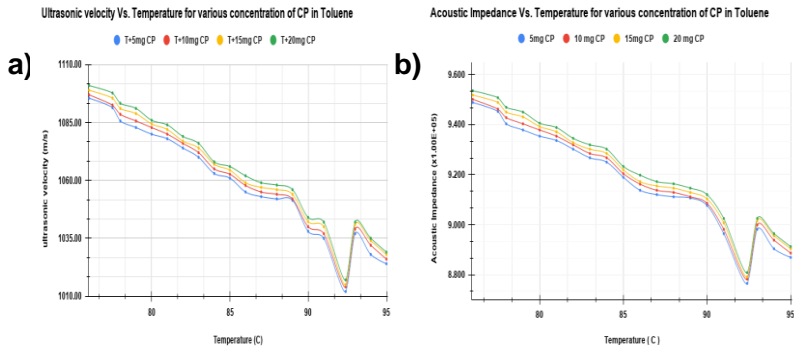


Fig. 3. Variation of a) ultrasonic velocity and b) acoustic impedance with temperature.

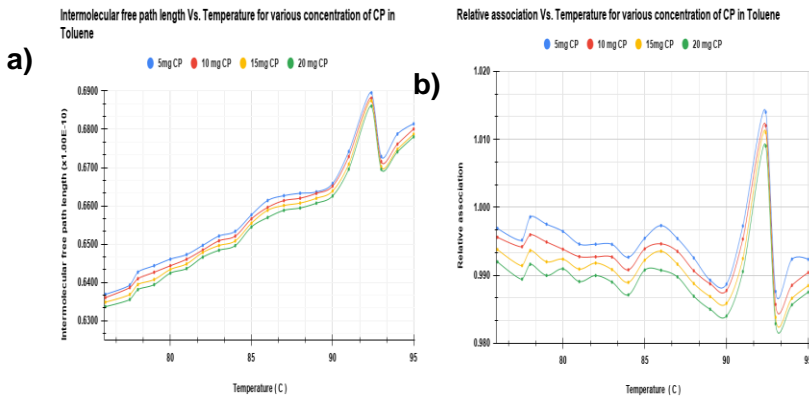


Fig. 4. Variation of a) intermolecular free length and b) relative association with temperature.

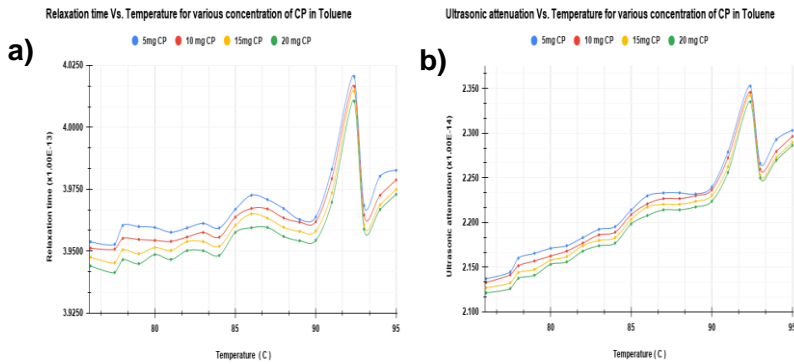


Fig. 5. Variation of a) relaxation and b) ultrasonic attenuation with temperature.

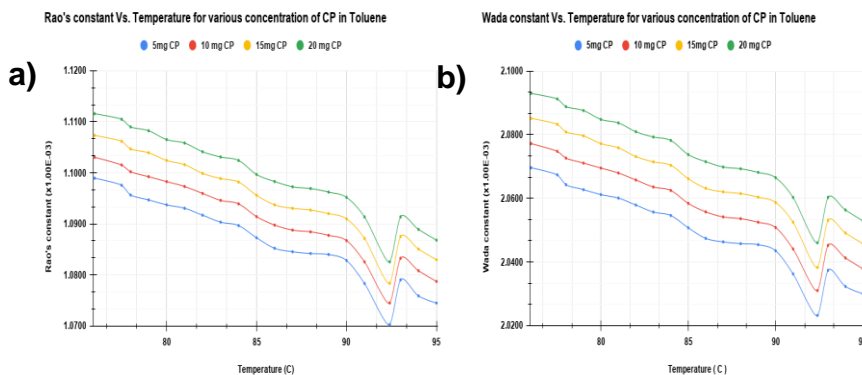


Fig. 6. Variation of a) Rao's constant and b) Wada constant with temperature.

5. Discussion

The variation of ultrasonic velocity with temperature (Fig. 3a) shows that the magnitude of ultrasonic velocity is greater in the anisotropic phase than that of in the isotropic phase. With an increase in temperature towards the phase transition temperature, ultrasonic velocity decreases. No noticeable peaks are observed for the smectic and blue phase; however, a sharp dip in the ultrasonic velocity is seen at the clearing point. With the decrease in the degree of order of molecules in the isotropic phase, inter-molecular free path length increases and ultrasonic velocity decreases at the clearing temperature. This graph also suggests that the ultrasonic velocity of the sample increases with the concentration of the cholesteric liquid crystal.

Acoustic impedance is directly proportional to the ultrasonic velocity of the mixture. Just like ultrasonic velocity, it decreases with the temperature rise but increases with the increase in the concentration of CLC. It also shows an abrupt dip at the clearing point (Fig. 3b).

The speed of ultrasonic waves in the solutions depends on the variation of inter-molecular free path length. The increase or decrease in free length suggests weakening and strength of intermolecular attraction. The graphical variation of intermolecular free length with temperature (Fig. 4a) shows that it increases with temperature rise but decreases with an increase of concentration of CLC. The ultrasonic velocity increases due to the increases in concentration; therefore, the inter-molecular free path length has to decrease with the increase in concentration and vice-versa [14].

Relative association (RA) is the property that deals with the interaction between solute and solvent. In our analysis, the values of relative association (Fig. 4b) decrease with an increase in the concentration of CLC due to the breaking up of toluene (solvent) molecules on the addition of CP (solute).

The relaxation time and ultrasonic attenuation (Fig. 5a,b) decrease with increasing concentration. One of the factors responsible for variation in ultrasonic attenuation and relaxation time in liquids is a viscous loss. As concentration increases, ultrasonic velocity

and viscosity increase. Hence relaxation time and ultrasonic attenuation decrease with the concentration of cholesteryl pelargonate. Both the graph shows anomalous behavior at clearing temperature.

The Rao's constant and Wada constant (Figs. 6a,b) increases with the rise in concentration. This supports the strong interaction of solute-solvent molecules in the CLC solutions. These variations in the acoustic parameters of cholesteric liquid crystal suggest that there are strong CLC-solvent interactions at clearing temperature. Due to solute-solvent interactions, the structure of the CLC is modified to a considerable extent.

6. Conclusion

The ultrasonic technique is a powerful tool for the investigation of acoustical parameters of crystal mixtures. These parameters can be used to establish the type of molecular interaction between solute and solvent, the knowledge of which is essential in the technological applications of the materials. The ultrasonic velocity of CLC slightly deviates from its linear trend in the anisotropic region at most of the phase transition temperatures detected by FPSS. This deviation of ultrasonic velocity with temperature can be used to predict the phase transition temperatures of CLC. The acoustical parameters depend both on the temperature and concentration of CLC and show anomalous behavior at the clearing temperature suggesting structural modification in the liquid crystal. These modifications in the molecular alignment have applications in displays, sensors, and thermal imaging. The present study describes the acoustical properties that confirm the molecular interaction of Cholesteryl Pelargonate with the solvent toluene.

Future research directions

The blue phases are stable only for a narrow temperature range, this characteristic hinders their applicability. However, the temperature range can be widened and stabilized by mixing nanoparticles in the CLC [19].

For practical applications, the clearing point of CP (92.4 °C) has to be lowered down towards room temperature by introducing suitable external dopants.

Acknowledgment

The author acknowledges the University of Mumbai, India for funding a Minor Research Grant Project (2019) which supported me to perform my work (Research Project number-395).

References

1. S. Singh, *Liquid Crystals: Fundamentals* (World Scientific, 2002).
<https://doi.org/10.1142/4369>
2. X. Xu, Y. Liu, and D. Luo, *Liq. Crys.* **47**, 399 (2020).
<https://doi.org/10.1080/02678292.2019.1655170>

3. R. Manda, S. Pagidi, Y. Heo, Y. J. Lim, M. S. Kim, and S. H. Lee, NPG Asia Mater. **12**, 1 (2020). <https://doi.org/10.1038/s41427-020-0225-8>
4. A. Devi, P. Malik, and H. Kumar, J. Mol. Liq. **214**, 145 (2016). <https://doi.org/10.1016/j.molliq.2015.11.025>
5. S. Mani, M. Pradhan, A. Sharma, S. Hadkar, K. Mishra, J. Amare, and P. Sarawade, Non-metallic Mater. Sci. **2**, ID 1821 (2020). doi.org/10.30564/omms.v2i1.1821
6. I. Gabrielli and L. Verdini, Nuovo Cim. **2**, 526 (1955). <https://doi.org/10.1007/BF02826512>
7. J. R. Otia and A. R. K. L. Padmini, Mol. Cryst. Liq. Cryst. **36**, 25 (1976). <https://doi.org/10.1080/00268947608084828>
8. S. K. Kor, A.K. Srivastava, and R.P. Khare, Nuovo Cim. D **2**, 1254 (1983). <https://doi.org/10.1007/BF02460210>
9. A. Kanwar and P. Mhatre, Int. J. Eng. Res. Tech. **3**, 2080 (2014).
10. J. P. Singh and R. Sharma, Int. J. Eng. Res. Develop. **5**, 48 (2013).
11. J. V. Rao and C. R. K. Murty, Zeitschrift für Naturforschung A **36**, 1002 (1981). <https://doi.org/10.1515/zna-1981-0913>
12. K. R. K. Rao, J. V. Rao, J. V. P. Venkatacharyulu, and V. Baliah, Mol. Cryst. Liq. Cryst. **136**, 307 (1986). <https://doi.org/10.1080/00268948608074732>
13. J. P. Singh and R. Sharma, IOSR J. Appl. Phys. **3**, 88 (2013). <https://doi.org/10.9790/4861-0358891>
14. S. S. Kulkarni and U. V. Khadke, Ind. J. Mat. Sci. ID 9582582 (2016). <https://doi.org/10.1155/2016/9582582>
15. A. Kanwar, J. Optics **36**, 31 (2007). <https://doi.org/10.1007/BF03354814>
16. A. Kanwar, J. G. Sureshchandra, S. Patil, and G. B. Vakil, J. Optics **37**, 9 (2008). <https://doi.org/10.1007/BF03354832>
17. S. A. Mani, J. R. Amare, S. U. Hadkar, K. G. Mishra, M. S. Pradhan, H. Al-Johani, and P. B. Sarawade, Mol. Cryst. Liq. Cryst. **646**, 183 (2017). <https://doi.org/10.1080/15421406.2017.1287478>
18. R. A. Gharde and S. Y. Thakare, Int. J. Sci. Res. **4**, 2690 (2015).
19. E. Karatairi, B. Rožič, Z. Kutnjak, V. Tzitzios, G. Nounesis, G. Cordoyiannis, J. Thoen, C. Glorieux, and S. Kralj, Phys. Rev. E **81**, 041703 (2010). <https://doi.org/10.1103/PhysRevE.81.041703>